Cite this article
Baker CJ and Soper D
Calculation of the overturning wind speed of large road vehicles at exposed sites.
Proceedings of the Institution of Civil Engineers – Transport,
https://doi.org/10.1680/jtran.18.00102

Research Article
Paper 1800102
Received 03/07/2018;
Accepted 10/12/2018

Keywords: bridges/risk & probability analysis/wind loading & aerodynamics

Transport

ice Publishing

Calculation of the overturning wind speed of large road vehicles at exposed sites

Chris J. Baker MA, PhD, FICE, FIHT, FRMetS, FHEA
Professor, School of Engineering, University of Birmingham, Birmingham, UK (corresponding author: c.j.baker@bham.ac.uk) (Orcid:0000-0001-7572-1871)

David Soper MSc, PhD
Lecturer, School of Engineering, University of Birmingham, Birmingham, UK (Orcid:0000-0003-0889-2317)

High-sided vehicles are particularly vulnerable to high wind conditions and at sites that are regarded as vulnerable, a range of vehicle restrictions are imposed in high winds. These may include vehicle speed reductions or complete restrictions on the movement of different categories of vehicle at different wind gust speeds. This paper builds on earlier work that has been carried out and seeks to develop a simple but conservative method that can be used to specify vehicle restriction strategies. This is based on a collation of a wide range of data for aerodynamic rolling moment coefficients that allows a simple parameterisation to be developed. This is then used in an overturning model to develop a non-dimensional relationship between overturning gust speed and vehicle speed. The parameter used in the non-dimensionalisation is a characteristic wind speed that is a function of vehicle weight and geometry, and effectively specifies the vulnerability of the vehicle to overturning in high winds. Dimensional relationships between overturning gust velocities and vehicle velocities can thus be derived for different vehicle types and used to develop site-specific vehicle restriction methods.

Notation

A	reference area (m^2)
$C_{RL}(30)$	leeward wheel rolling moment coefficient at $\psi = 30°$
$C_{RL}(\psi)$	leeward wheel rolling moment coefficient at $\psi°$
$\boldsymbol{c}$	characteristic velocity (m/s) – Equation 7
$\boldsymbol{g}$	acceleration due to gravity (m/s^2)
H	vehicle height (m)
h	reference height (m)
L	vehicle length (m)
M	vehicle mass (kg)
p	wheel base semi-width (m)
$\boldsymbol{R}_L$	leeward wheel rolling moment (Nm)
$\boldsymbol{u}$	wind gust velocity (m/s)
$\bar{u}$	$\boldsymbol{u}/\boldsymbol{c}$
$\boldsymbol{u}_i$	wind gust velocity at which overturning occurs (m/s)
$\bar{u}_i$	$\boldsymbol{u}_i/\boldsymbol{c}$
$\boldsymbol{V}$	wind velocity relative to vehicle (Equation 3) (m/s)
$\bar{V}$	$\boldsymbol{V}/\boldsymbol{c}$
$\boldsymbol{v}$	vehicle velocity (m/s)
$\bar{v}$	$\boldsymbol{v}/\boldsymbol{c}$
α	proportion of wheel unloading
β	wind direction relative to vehicle direction of travel (degrees)
ρ	density of air (kg/m^3)
ψ	yaw angle (Equation 4) (degrees)

1. Background

High-sided road vehicles are prone to overturning in high winds, particularly when they are unladen, and there are frequent news reports of such incidents (e.g. BBC, 2015, 2017a, 2017b). Safety considerations thus often make it necessary to place restrictions on the movement of road traffic during wind storms at sites such as long-span bridges or exposed embankment sites. These restrictions can range from speed limits for different vehicle types to complete closure of the road to vehicles of all types. For example, on Queensferry Bridge in Scotland (which will be considered further later in the paper)

- a blanket speed restriction of 40 mph (~64 km/h) is put into place when wind gusts are above 50 mph (22·4 m/s)
- double-deck buses are not allowed to travel over the bridge for gust speeds higher than 60 mph (26·8 m/s)
- high-sided vehicles are banned from crossing when wind gust speeds exceed 70 mph (31·3 m/s)
- all traffic except cars is stopped for gusts above 90 mph (40·3 m/s)
- the bridge is closed when gust speeds reach 100 mph (44·7 m/s) (FBU, 2018).

Similarly, restrictions on vehicle movements can sometimes be required in urban areas where ground-level wind speeds around high-rise buildings can be sufficient to cause vehicle overturning incidents (BBC, 2014).

There have been a number of investigations into the effects of cross-winds on road vehicles in the past. Clearly, the most basic information that is required is knowledge of the cross-wind forces and moments on vehicles. Wind tunnel measurements of these forces for a variety of different vehicle types have been reported by Baker (1988), Coleman and Baker (1990), Sterling *et al.* (2010), Cheli *et al.* (2011a, 2011b); Dorigatti *et al.* (2012), Han *et al.* (2014) and Liu *et al.* (2016), with data given for vehicles on flat ground, bridge, embankment and viaduct scenarios. In addition, Haan *et al.* (2017) report measurements on vehicle forces in a tornado vortex

generator and Xiang *et al.* (2017) describe measurements made using a moving model facility. Computational fluid dynamics (CFD) calculations of cross-wind forces have been reported (e.g. Sterling *et al.*, 2010; Stoyanoff *et al.*, 2015). As is the case in most sectors of wind engineering, full-scale data with which to compare wind tunnel and CFD measurements are understandably sparse and the only investigations of this type known to the author are those of Sterling *et al.* (2010) for a stationary vehicle.

At this point, it should also be noted that a number of tests have also been carried out to investigate transient wind effects on vehicles as they pass bridge pylons (Argentini *et al.*, 2011; Rocchi *et al.*, 2012; Wang and Xu, 2015). However, this particular issue is beyond the scope of the method presented in this paper and will not be addressed further here.

With cross-wind forces having been obtained, some method is required to translate these forces into a wind speed level that will result in an accident. Methods for such a procedure were first derived by Baker in the 1980s using simple static analytical models of vehicle behaviour, with and without human driving input (Baker, 1986, 1987, 1991); critical wind conditions for vehicle sideslip and rollover incidents were determined. Snæbjörnsson *et al.* (2007) put the analysis into a probabilistic framework that enabled an accident index to be defined for certain levels of accident probability. This approach was taken further and refined somewhat by Batista and Perkovič (2014), and Kim *et al.* (2016) used the latter's methodology to calculate the risk of a wind-induced accident on a long-span bridge. Cheli *et al.* (2006) used a more complex dynamic vehicle/driver model of a vehicle and its suspension in simulated fluctuating wind conditions to evaluate vehicle forces and path. This approach was further developed by Zhou and Chen (2015) and Chen *et al.* (2015) who both described a complex calculation linking fluctuating wind conditions, the dynamic behaviour of vehicles and the dynamic behaviour of bridges. Finally, mention should be made of the work of Maruyama and Yamazaki (2006) who used a more complex version of the original static analysis and, interestingly, incorporated human driver behaviour by inputting the cross-wind model into a driver simulator, thus introducing real human involvement.

On many long-span bridges and other exposed sites, wind barriers of different sorts are used to protect traffic from high winds and to increase the wind gust speeds at which traffic restrictions need to be put in place. These barriers are usually designed using wind tunnel tests and the level of shelter is usually quantified by a reduction in the forces and moments on the vehicle (e.g. Alonso-Estebanez *et al.*, 2017; Chen *et al.*, 2015; Chu *et al.*, 2013; Dorigatti *et al.*, 2012). However, these force and moment measurements are not always related to the values of wind speed that may result in an accident and to the risk of such accidents.

Ultimately, the problem that arises when applying the results of the above research is that the real-life situation at any one site is complex, with a wide range of different vehicle types, sizes, weights and levels of vulnerability, with wind approaching from a range of directions. In addition, many of the methods outlined above (including those of the author) are practically difficult and time-consuming to use. Operationally, any traffic restrictions need to be quite simple and easy to implement, and must be aimed at protecting the most vulnerable types of traffic at the site. Complex methodologies are thus not always easy to use in practical situations, although they can be useful in calibrating simpler methods. In addition, it will be seen from what follows that there can be considerable uncertainty in the aerodynamic forces and moments, with large differences between the results of nominally similar wind tunnel tests or CFD calculations.

The work presented in this paper steps back from recent developments in the field in some ways and sets out a methodology for assessing safe wind speeds for vehicles in high cross-winds that, while as rigorous as possible, is deliberately simple and in a form that can be easily used by bridge operators and transport authorities, both in the planning and design stage for new infrastructure and operationally when considering whether restrictions need to be applied. The methodology is outlined in Section 2 and the specification of aerodynamic force and moment coefficients is considered in Section 3. An analysis that relates these coefficients to accident wind speeds is given in Section 4 and the application of this analysis is set out in Section 5. Section 6 considers how this methodology can be used in wider contexts of risk assessment. Some concluding remarks are made in Section 7.

2. Outline of methodology

The methodology adopted is as follows.

- Only the most common and serious type of wind-induced accident is considered – the rollover of large vans, lorries and other similar vehicles. Such events dominate the accident statistics, as exemplified in the description of the 1991 Burns Night storm in the UK (Baker and Reynolds, 1991) where this type of overturning incident accounted for 47% of all injurious accidents. Sideslip accidents (vehicles blown to one side without overturning) only contributed to around 19% of the total number of accidents. Most of the other accidents involved vehicles colliding with trees or other debris blown onto the road. Thus, of the accidents directly caused by strong winds, around 70% are of the rollover type.
- Accidents are assumed to occur when the vertical reaction at the windward wheels becomes zero and the vehicle is assumed to overturn as a solid body.
- The wind speeds that result in such accidents are fully specified by a 1–3 s gust speed.

- Data for the aerodynamic parameter of relevance to this situation – the rolling moment about the leeward wheels – were collated from a range of investigations and a simple parameterisation is suggested that is a reasonable and largely conservative representation of the experimental results.
- A simple rollover analysis is set out that allows a non-dimensional cross-wind characteristic function to be determined – non-dimensional overturning wind speed as a function of wind direction and non-dimensional vehicle speed.
- The non-dimensionalisation of velocities is carried out through the use of a characteristic velocity that defines the rollover characteristics of the vehicle.
- Both non-dimensionalised and dimensional curves of accident wind speed plotted against vehicle velocity can then be determined, which can be used to specify vehicle and wind speed restrictions at specific sites.

3. Overturning moment coefficients

The overturning moment on a vehicle about the leeward wheels, $\boldsymbol{R}_{\mathrm{L}}$, can be specified by the overturning moment coefficient C_{RL}

$$1. \quad C_{\mathrm{RL}} = \frac{\boldsymbol{R}_{\mathrm{L}}}{0{\cdot}5\rho A h \boldsymbol{V}^2}$$

where A is a reference area and h is a reference height, ρ is the density of air and $\boldsymbol{V}$ is the wind velocity relative to the vehicle.

Rolling moment coefficients are usually measured from static wind tunnel tests, as a function of yaw angle ψ (the wind angle relative to the vehicle), although other sorts of physical model test (tornado vortex generators or moving models) have been used, as have CFD calculations and, to a very limited degree, full-scale tests. A collation of data from a range of experiments for flat ground and unobstructed bridge scenarios is given in Figure 1, plotted in the form of $C_{\mathrm{RL}}(\psi)/C_{\mathrm{RL}}(30)$ where $C_{\mathrm{RL}}(30)$ is the rolling moment coefficient at a yaw angle of 30°. The figure includes data from most of the investigations outlined in Section 1, although potentially useful data from the work of Han *et al*. (2014) and Liu *et al*. (2016) could not be used because not all the relevant dimensions of the vehicles are given in those publications. It can be seen that the data collapse tolerably well when plotted in this way, at least in the lower yaw angle range, and can be conservatively represented by the simple curve

$$2. \quad \frac{C_{\mathrm{RL}}(\psi)}{C_{\mathrm{RL}}(30)} = \frac{\sin(\psi)}{\sin(30)}$$

This is a slight modification needed to the method used by Baker (2013) for cross-wind forces on trains, where the reference yaw angle is taken as 40° and a rather more complex

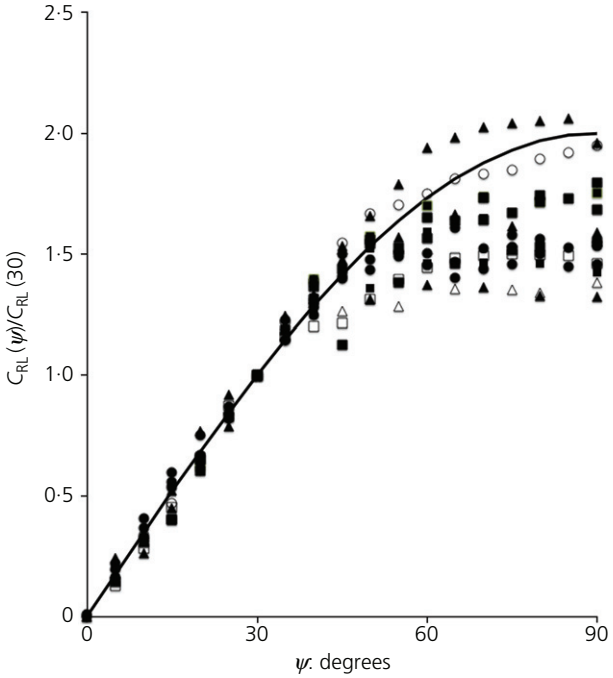

Figure 1. Collation of leeward wheel rolling moment characteristic data. Filled squares – articulated lorry with cab and container or box on trailer: Baker (1988), 1/25th low turbulence; Coleman and Baker (1990), 1/50th low turbulence, 1/50th turbulence, 1/50th boundary layer; Cheli *et al*. (2011b), 1/10th low turbulence; Dorigati *et al*. (2012), 1/40th boundary layer. Filled circles – long box lorry with four or more axles: Cheli *et al*. (2011a), 1/10th low turbulence, 1/10th turbulence; Cheli *et al*. (2011b), in combination with trailer, 1/10th low turbulence. Filled triangles – short box lorry with two or three axles: Sterling *et al*. (2010), full-scale boundary layer, 1/10th boundary layer, CFD boundary layer. Open squares – cab articulated with tanker trailer: Cheli *et al*. (2011b) 1/10th low turbulence. Open circles – trailer in combination with long box lorry: Cheli *et al*. (2011b) 1/10th low turbulence. Open triangles – double-deck bus: Dorigatti *et al*. (2012), 1/40th boundary layer. Solid line – curve fit

curve fit is found. Note that the values for most of the experiments diverge from the simple curve for yaw angles greater than 50°, with the main exception being the results of the full-scale experiments conducted by Sterling *et al*. (2010) (the filled triangles). The authors would argue that primacy should be given to such results, which represent some sort of ground truth, and thus the simple curve of Equation 2, which is a reasonable representation of these results, is appropriate. Nonetheless, the full-scale data have much scatter that is not apparent from the results shown, but which again suggests that a simple, conservative approach is appropriate.

The rolling moment coefficients at a yaw angle of 30° are listed in Table 1. Two sets of coefficients are given – the first is based on $A = 10$ m^2 and $h = 3$ m (which are conventional, nominal values) and the second is based on values of A given by the product of the overall vehicle length L and overall vehicle

Table 1. Collation of leeward wheel rolling moment coefficient data

Vehicle type	Simulation[a] and scale	L: m	H: m	$C_{RL}(30)$ $A = 10$ m^2 $h = 3$ m	$C_{RL}(30)$ $A = LH$ $h = H$
Baker (1988)					
Articulated lorry	LT, 1/25th	13·5	3·8	3·39	0·52
Coleman and Baker (1990)					
Articulated lorry	LT, 1/50th	13·5	3·8	2·63	0·41
	HT, 1/50th			2·81	0·43
	BL, 1/50th			3·31	0·51
Sterling *et al*. (2010)					
Short box lorry	BL, full-scale	6	3·5	0·75	0·31
	BL, 1/10th			0·96	0·39
	BL, CFD			0·94	0·38
Cheli *et al*. (2011a)					
Long box lorry	LT, 1/10th	7·8	3·5	1·15	0·36
	HT, 1/10th			1·21	0·38
Cheli *et al*. (2011b)					
Long box lorry combination with trailer	LT, 1/10th	7·8	3·5	1·23	0·39
Trailer combination with long box lorry	LT, 1/10th	7·6	4	1·38	0·34
Cab/tanker	LT, 1/10th	14·0	3·7	1·27	0·20
Articulated lorry	LT, 1/10th	14·0	3·8	2·16	0·31
Dorigatti *et al*. (2012)					
Double-deck bus	BL, 1/40th	10·1	4·4	2·80	0·43
Articulated lorry	BL, 1/40th	16·6	3·8	3·15	0·48

[a]LT, low-turbulence simulation; HT, high-turbulence simulation; BL, boundary layer simulation

height H, and values of h given directly by H. The first values show a steady increase in the coefficient with the length of the vehicle for all the sharp-edged vehicles, as would be expected, but the value for the cab/tanker (without sharp edges in the cross-section) is lower than would be expected for its length. Again, with exception of the cab/tanker, the values of the second set are almost all within the range 0·30–0·50, with the values for a short box lorry being 0·31–0·38, those for a long box lorry in the range 0·36–0·39 and those for an articulated lorry being between 0·41–0·52 (with the exception of the results of Cheli (2011b), which lie significantly below this range). These ranges thus indicate the level of uncertainty attached to any estimation of rolling moment coefficients obtained experimentally or computationally.

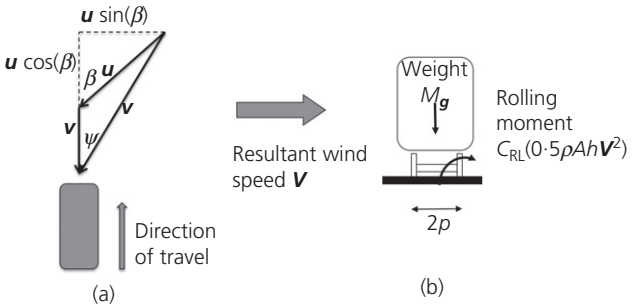

Figure 2. Velocities and rolling moments: (a) velocity vectors; (b) static model

4. Accident wind speed calculation

From the velocity vector diagram shown in Figure 2(a), it can be seen that if a vehicle is moving at a velocity $\boldsymbol{v}$ with a cross-wind of velocity $\boldsymbol{u}$ at a direction β to the direction of travel, then the wind velocity relative to the vehicle $\boldsymbol{V}$ is given by

$$3. \quad \boldsymbol{V}^2 = [\boldsymbol{u}\cos(\beta) + \boldsymbol{v}]^2 + [\boldsymbol{u}\sin(\beta)]^2$$

The wind direction relative to the vehicle, the yaw angle ψ, is given by

$$4. \quad \tan(\psi) = \frac{\boldsymbol{u}\sin(\beta)}{\boldsymbol{u}\cos(\beta) + \boldsymbol{v}}$$

Now, if one assumes that the critical condition occurs when the windward wheel reaction falls to zero, a simple static analysis (Figure 2(b)) gives the expression

$$5. \quad C_{RL}(0·5\rho AhV^2) = Mgp$$

where M is the vehicle mass and p is the semi-wheel base. In practice, a certain proportion (α) of wheel unloading (say 0·9) is often taken as the critical condition, giving the modified expression

$$C_{RL}(0·5\rho AhV^2) = \alpha Mgp$$

The wheel unloading proportion α may also be interpreted as a parameter that represents the dynamic effects of the vehicle suspension in the overturning process, or simply as a safety factor. From the above expressions it is possible to derive the dimensionless relationship

$$6. \quad [\bar{v}^2 + \bar{u}_i^2 + 2\bar{u}_i\bar{v}\cos(\beta)][\bar{u}_i\sin(\beta)]^2 = 1$$

where $\bar{v} = \boldsymbol{v}/\boldsymbol{c}$ and $\bar{u}_i = \boldsymbol{u}_i/\boldsymbol{c}$ in which $\boldsymbol{u}_i$ is the wind velocity at which an overturning incident will occur and $\boldsymbol{c}$ is the characteristic velocity given by

$$7. \quad \boldsymbol{c} = \sqrt{\frac{\alpha M \boldsymbol{g} p}{\rho C_{RL}(30) A h}}$$

Equation 6 gives the relationship between the dimensionless cross-wind speed needed for an overturning incident to occur, the wind direction and the dimensionless vehicle speed, with the vehicle parameters being fully specified by the characteristic velocity. It is completely general and can be applied to all vehicles and situations where the assumptions set out in Section 2 apply. It is also very simple in form, although it can only be solved analytically for very specific cases. This will be seen to be its major utility.

5. Application of methodology

Figure 3 shows the variation of the normalised overturning wind speed $\bar{u}_i$ with wind direction β for a variety of normalised vehicle speeds $\bar{v}$. The curves show a minimum value for values of $\bar{u}_i$ between 70° and 90°. Note that the curve for zero velocity has a minimum value of 1·0 at $\beta = 90°$ (i.e. pure cross-flow). In these conditions, $\boldsymbol{u}_i = \boldsymbol{c}$ and thus the characteristic velocity can be interpreted as the accident gust speed for a stationary vehicle normal to the wind direction. Figure 4

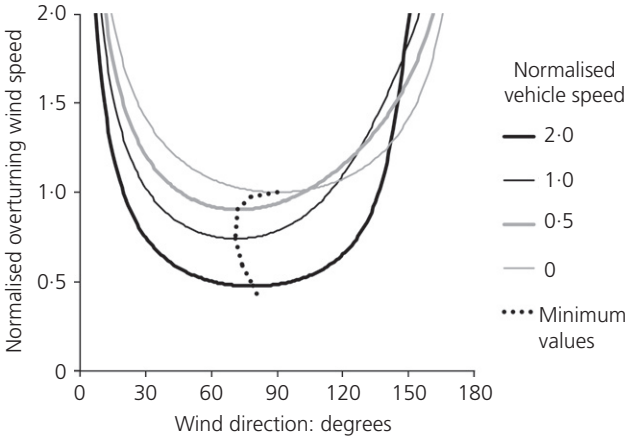

Figure 3. Non-dimensional overturning wind speed plotted against wind direction for a range of non-dimensional vehicle velocities

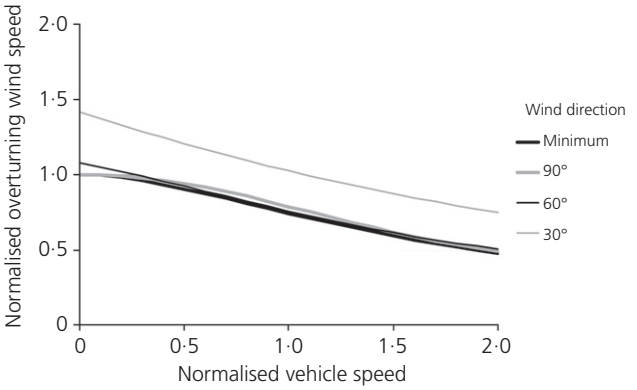

Figure 4. Non-dimensional overturning wind speed plotted against non-dimensional vehicle velocities for minimum values and different wind direction values

shows the variation of this minimum value with normalised vehicle speed. This figure shows the normalised overturning wind speeds plotted against vehicle speeds, which are appropriate to situations where the wind direction is very variable or unknown, and thus the minimum value is the appropriate value to use. Curves are also given for values of $\bar{u}_i$ at wind directions of 30°, 60° and 90°, which may be useful if the wind direction can be more accurately specified. It can be seen that there is little difference between the curve for the minimum values and those for wind directions of 60° and 90°, but the 30° curve is significantly higher. It will be shown later in the paper that if the wind direction can be confidently predicted to be along the vehicular direction of travel, wind speed and vehicle speed restrictions could be relaxed.

The curve for the minimum values in Figure 4 can be given, to a good approximation, by the very simple expression

$$8. \quad \bar{u}_i = e^{-(\bar{v}/2{\cdot}4)^{1{\cdot}41}}$$

and that for the 30° wind direction case is provided by the equally simple expression

$$9. \quad \bar{u}_i = 1{\cdot}41e^{-(\bar{v}/3)^{1{\cdot}05}}$$

These formulae are wholly empirical curve fits and have no physical meaning, but their Weibull-like forms are somewhat satisfying for wind engineering practitioners.

The above analysis has been expressed in dimensionless terms and, as such, can give generalised formulae applicable to a range of situations. In practical terms, however, it is useful to express the results in dimensional terms. To do this, values of the characteristic velocity $\boldsymbol{c}$ are required. Typical values of this parameter are given in Table 2 for a small number of vehicle

Table 2. Calculation of characteristic velocities

							c: m/s	
	Unladen mass: kg	Laden mass: kg	*L*: m	*H*: m	*p*: m	$C_{RL}(30)$	Unladen	Laden
Small box lorry	7000	16 000	8·0	3·5	1·2	0·4	40·2	60·8
Large box lorry	9000	18 000	12·0	3·5	1·2	0·4	37·2	52·7
Articulated lorry	16 000	40 000	15·0	4·0	1·2	0·5	34·3	54·2
Double-deck bus	10 000	14 000	12·0	4·4	1·2	0·4	29·7	35·2

categories for which aerodynamic information is available. Representative values of the weights and dimensions are assumed. It can be seen that, for unladen vehicles, the values of c are between 30 m/s and 40 m/s, with the laden values being very much higher. Figure 5 thus shows the variation of the minimum value of the overturning wind speed for all wind directions plotted against vehicle speed for $c = 30$, 35 and 40 m/s. The vehicle and wind speeds are both given in the units of miles per hour, which is of course scientifically non-standard, but these are the units actually used in practice in the UK and USA (10 mph $\approx$ 16 km/h). The figure also shows the vehicle restriction limits for Queensferry Bridge in Scotland outlined in Section 1, although only those for double-deck buses and high-sided vehicles are relevant to the current methodology (Section 1). These limits ensure that the $c = 30$ m/s line and $c = 35$ m/s line are not crossed by buses and high-sided vehicles, respectively, which seems very sensible in the light of the values of c given in Table 2. The analysis and the operational experience of this particular bridge are thus in reasonable agreement.

Finally, Figure 6 shows the wind speeds for vehicle overturning for the minimum values and the minimum values for wind

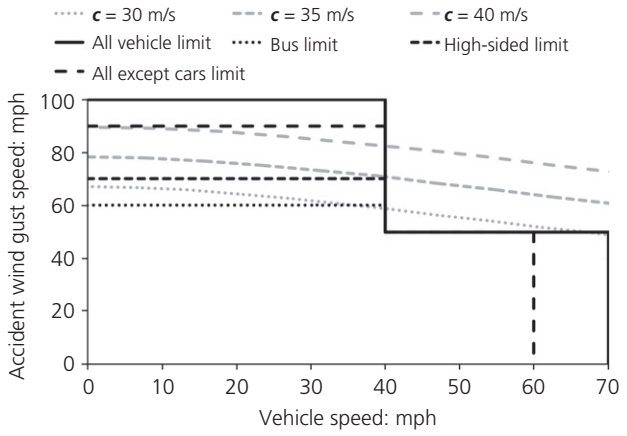

Figure 5. Minimum overturning wind speed for all wind directions plotted against vehicle speed for $c = 30$, 35 and 40 m/s and Queensferry Bridge limits for different vehicle categories (vertical lines at 60 and 70 mph indicate national speed limits for different vehicle classes)

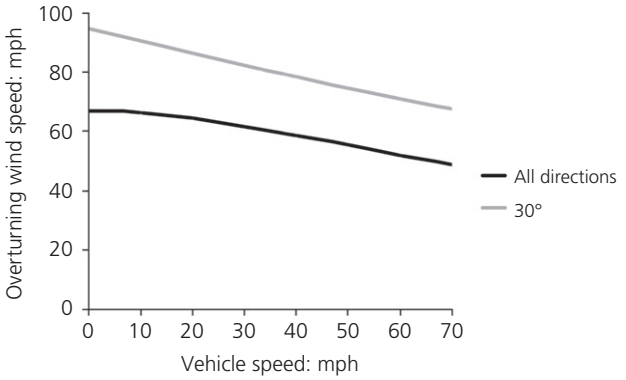

Figure 6. Overturning wind speed plotted against vehicle speed for all wind directions and 30° wind direction, for $c = 30$ m/s

directions of less than 30° to the vehicle direction of travel. The latter can be seen to be significantly higher than the former, showing the potential for relaxing wind and vehicle speed limits if the wind direction is known to be predominantly along the roadway.

6. Use of the methodology

The analysis presented gives a straightforward way of determining appropriate wind gust speed limits at exposed sites. The method is as follows.

- Determine the different vulnerable vehicle types that will use the site in terms of size and weight, and calculate values of the characteristic velocity c for each vehicle type.
- Determine either the lowest value of c for all traffic as the basis of vehicle restrictions or divide the vehicles into easily identifiable categories for which it is practical to apply category-specific restriction methods, with a value of c for each.
- If the directions of strong winds are very variable, determine the accident wind speed/vehicle speed characteristic from Equation 8 for each vehicle category.
- If there are identifiable periods when the wind direction will be predominantly along the roadway, determine the wind speed/vehicle speed characteristic from Equation 9 for each vehicle category for that case.
- Devise suitable, site-specific vehicle restrictions, such as those illustrated in Figure 6, so that the operational

conditions lie below the wind speed/vehicle speed characteristics at all times.

If the site is protected with wind fences, this will result in a lower value of $C_{RL}(30)$ and thus a higher value of the characteristic velocity c. Equation 8 can then be used to determine vehicle restrictions with such protection in place or, alternatively, can be used to give a target value of the rolling moment coefficient that the protection should achieve.

The methodology could also potentially be used by vehicle manufacturers, who could use calculated values of c to give an indication of the cross-wind stability of their vehicle designs. This could involve 'tuning' of the value of the parameter α through modification of suspension parameters. Highway authorities could also easily incorporate the curves given by Equation 8 into a route risk analysis, taking into account vehicle types and operational patterns and the gust wind speeds at sites along the route, which could be specified by the Weibull distribution format set out by Baker (2015).

7. Concluding remarks

A simple method that can be used in the specification of road vehicle restrictions at exposed sites during windy periods has been presented. A very simple, conservative approach was deliberately taken in order to produce a methodology that is very straightforward to use in practice. However, the more complex static and dynamic methodologies developed by the authors and by others still have a place, particularly for wind-sensitive sites or for complex geometries such as calculating the behaviour of vehicles as they move in and out of the shelter of bridge pylons. The following aspects of the simplified methodology are worthy of mention.

- A generalised formulation of an overturning wind characteristic that is valid for a wide range of vehicle types.
- The specification of individual vehicle vulnerability through the use of a characteristic velocity that can easily be calculated from weight and geometric parameters.
- A very simple formulation that relates dimensionless overturning wind speed to dimensionless vehicle velocity and can be used to specify vehicle restrictions at specific sites or incorporated into route-based risk calculations.

To enable the methodology to be used more widely, the prime need is for data for the leeward wheel rolling moment coefficients for a range of different vehicle types of relevance in different countries.

REFERENCES

Alonso-Estebanez A, Del Coz Díaz JJ, Ivarez Rabanal FPA and Pascual-Munoz P (2017) Performance analysis of wind fence models when used for truck protection under crosswind through numerical modelling. *Journal of Wind Engineering & Industrial Aerodynamics* **168**: 20–31, https://doi.org/10.1016/j.jweia.2017.04.021.

Argentini T, Ozkan E, Rocchi D, Rosa L and Zasso A (2011) Cross-wind effects on a vehicle crossing the wake of a bridge pylon. *Journal of Wind Engineering & Industrial Aerodynamics* **99(6–7)**: 734–740, https://doi.org/10.1016/j.jweia.2011.01.021.

Baker CJ (1986) A simplified analysis of various types of wind induced road vehicle accidents. *Journal of Wind Engineering & Industrial Aerodynamics* **22(1)**: 69–85, https://doi.org/10.1016/0167-6105(86)90012-7.

Baker CJ (1987) Measures to control vehicle movement at exposed sites during windy periods. *Journal of Wind Engineering & Industrial Aerodynamics* **25(2)**: 151–167, https://doi.org/10.1016/0167-6105(87)90013-4.

Baker CJ (1988) High sided articulated lorries in strong cross winds. *Journal of Wind Engineering & Industrial Aerodynamics* **31(1)**: 67–85, https://doi.org/10.1016/0167-6105(88)90188-2.

Baker CJ (1991) Ground vehicles in high cross winds – part 3: the interaction of aerodynamic forces and the vehicle system. *Journal of Fluids and Structures* **5(2)**: 221–241, https://doi.org/10.1016/0889-9746(91)90478-8.

Baker CJ (2013) A framework for the consideration of the effects of crosswinds on trains. *Journal of Wind Engineering & Industrial Aerodynamics* **123(Part A)**: 130–142, https://doi.org/10.1016/j.jweia.2013.09.01.

Baker CJ (2015) Risk analysis of pedestrian and vehicle safety in windy environments. *Journal of Wind Engineering & Industrial Aerodynamics* **147**: 283–290, https://doi.org/10.1016/j.jweia.2015.10.001.

Baker CJ and Reynolds S (1991) Wind induced accidents of road vehicles. *Accident Analysis and Prevention* **24(6)**: 559–575, https://doi.org/10.1016/0001-4575(92)90009-8.

Batista M and Perkovič M (2014) A simple static analysis of moving road vehicle under crosswind. *Journal of Wind Engineering & Industrial Aerodynamics* **128**: 105–113, https://doi.org/10.1016/j.jweia.2014.02.009.

BBC (British Broadcasting Corporation) (2014) Bridgewater Place wind reduction plans unveiled. *BBC News*, 16 January. See https://www.bbc.co.uk/news/uk-england-leeds-25760733 (accessed 29/12/2018).

BBC (2015) Humber Bridge winds blow over lorry. *BBC News*, 31 March. See https://www.bbc.co.uk/news/uk-england-humber-32137694 (accessed 29/12/2018).

BBC (2017a) Strong winds in US topple truck on highway. *BBC News*, 11 February. See https://www.bbc.co.uk/news/av/world-us-canada-38940832/strong-winds-in-us-topple-truck-on-highway (accessed 29/12/2018).

BBC (2017b) Forth Road Bridge reopens after lorry blown over. *BBC News*, 11 January. See https://www.bbc.co.uk/news/uk-scotland-38575843 (accessed 29/12/2018).

Cheli F, Belforte P, Melzi S, Sabbioni E and Tomasini G (2006) Numerical–experimental approach for evaluating cross-wind aerodynamic effects on heavy vehicles. *Vehicle System Dynamics* **44(1)**: 791–804, https://doi.org/10.1080/00423110600886689.

Cheli F, Corradi R, Sabbioni E and Tomasini G (2011a) Wind tunnel tests on heavy road vehicles: cross wind induced loads – part 1. *Journal of Wind Engineering & Industrial Aerodynamics* **99(10)**: 1000–1010, https://doi.org/10.1016/j.jweia.2011.07.009.

Cheli F, Ripamonti F, Sabbioni E and Tomasini G (2011b) Wind tunnel tests on heavy road vehicles: cross wind induced loads – part 2. *Journal of Wind Engineering & Industrial Aerodynamics* **99(10)**: 1011–1024, https://doi.org/10.1016/j.jweia.2011.07.007.

Chen N, Lin Y, Wang B, Su Y and Xiang H (2015) Effects of wind barrier on the safety of vehicles driven on bridges. *Journal of Wind Engineering & Industrial Aerodynamics* **143**: 113–127, https://doi.org/10.1016/j.jweia.2015.04.021.

Chu CR, Chang CY, Huang CJ *et al.* (2013) Windbreak protection for road vehicles against crosswind. *Journal of Wind Engineering & Industrial Aerodynamics* **143**: 113–127, https://doi.org/10.1016/j.jweia.2013.02.001.

Coleman SA and Baker CJ (1990) High sided road vehicles in cross winds. *Journal of Wind Engineering & Industrial Aerodynamics* **36(2)**: 1383–1397, https://doi.org/10.1016/0167-6105(90)90134-X.

Dorigatti F, Sterling M, Rocchi D *et al.* (2012) Wind tunnel measurements of crosswind loads on high sided vehicles over long span bridges. *Journal of Wind Engineering & Industrial Aerodynamics* **107–108**: 214–224, https://doi.org/10.1016/j.jweia.2012.04.017.

FBU (Forth Bridges Unit) (2018) *Wind and Weather*. FBU, South Queensferry, UK. See https://www.theforthbridges.org/plan-your-journey/wind-and-weather/ (accessed 29/12/2018).

Haan FL, Sarkar PP, Kopp GA and Stedman DA (2017) Critical wind speeds for tornado-induced vehicle movements. *Journal of Wind Engineering & Industrial Aerodynamics* **168**: 1–8, https://doi.org/10.1016/j.jweia.2017.04.014.

Han Y, Cai CS, Zhang J, Chen S and He X (2014) Effects of aerodynamic parameters on the dynamic responses of road vehicles and bridges under cross winds. *Journal of Wind Engineering & Industrial Aerodynamics* **134**: 78–95, https://doi.org/10.1016/j.jweia.2014.08.013.

Kim SJ, Yoo CH and Kim HK (2016) Vulnerability assessment for the hazards of crosswinds when vehicles cross a bridge deck. *Journal of Wind Engineering & Industrial Aerodynamics* **156**: 62–71, https://doi.org/10.1016/j.jweia.2016.07.005.

Liu X, Han Y, Cai CS, Levitan M and Nikitopoulos D (2016) Wind tunnel tests for mean wind loads on road vehicles. *Journal of Wind Engineering & Industrial Aerodynamics* **150**: 15–21, https://doi.org/10.1016/j.jweia.2015.12.004.

Maruyama Y and Yamazaki F (2006) Driving simulator experiment on the moving stability of an automobile under strong crosswind. *Journal of Wind Engineering & Industrial Aerodynamics* **94(4)**: 191–205, https://doi.org/10.1016/j.jweia.2005.12.006.

Rocchi D, Rosa L, Sabbioni E, Sbrosi M and Belloli M (2012) A numerical–experimental methodology for simulating the aerodynamic forces acting on a moving vehicle passing through the wake of a bridge tower under cross wind. *Journal of Wind Engineering & Industrial Aerodynamics* **104–106**: 256–265, https://doi.org/10.1016/j.jweia.2012.03.012.

Snæbjörnsson J, Baker CJ and Sigbjörnsson R (2007) Probabilistic assessment of road vehicle safety in windy environments. *Journal of Wind Engineering & Industrial Aerodynamics* **95(9–11)**: 1445–1462, https://doi.org/10.1016/j.jweia.2007.02.020.

Sterling M, Quinn A, Hargreaves D *et al.* (2010) A comparison of different methods to evaluate the wind induced forces on a high sided lorry. *Journal of Wind Engineering & Industrial Aerodynamics* **98(1)**: 10–20, https://doi.org/10.1016/j.jweia.209.08.008.

Stoyanoff S, Dallairea P, Zolib T and Daly G (2015) Vehicle roll-over stability in strong winds on long-span bridges. *Bridge Structures* **11(4)**: 149–162, https://doi.org/10.3233/BRS-160094.

Wang B and Xu Y (2015) Safety analysis of a road vehicle passing by a bridge tower under crosswinds. *Journal of Wind Engineering & Industrial Aerodynamics* **137**: 25–36, https://doi.org/10.1016/j.jweia.2014.11.017.

Xiang H, Li Y, Chen S and Li C (2017) A wind tunnel test method on aerodynamic characteristics of moving vehicles under crosswinds. *Journal of Wind Engineering & Industrial Aerodynamics* **163**: 15–23, https://doi.org/10.1016/j.jweia.2017.01.013.

Zhou Y and Chen S (2015) Fully coupled driving safety analysis of moving traffic on long-span bridges subjected to crosswind. *Journal of Wind Engineering & Industrial Aerodynamics* **143**: 1–18, https://doi.org/10.1016/j.jweia.2015.04.015.

How can you contribute?

To discuss this paper, please email up to 500 words to the editor at journals@ice.org.uk. Your contribution will be forwarded to the author(s) for a reply and, if considered appropriate by the editorial board, it will be published as discussion in a future issue of the journal.

Proceedings journals rely entirely on contributions from the civil engineering profession (and allied disciplines). Information about how to submit your paper online is available at www.icevirtuallibrary.com/page/authors, where you will also find detailed author guidelines.